Chapter 4 – Rate Constants of the CN + Benzene and CN + Toluene Reactions from 15 – 294 K, and Interstellar Implications

This chapter is reprinted and adapted with permission from J. Phys. Chem. A 2020, 124, 39, 7950–7958. Copyright 2020, American Chemical Society. Additional data is from Astrophys. J. Lett. 2020, 891:L41

4.1 – Abstract

CN is known for its fast reactions with hydrocarbons at low temperatures, but relatively few studies have focused on the reactions between CN and aromatic molecules. The recent detection of benzonitrile in the interstellar medium, believed to be produced by the reaction of CN and benzene, has ignited interest in studying these reactions. Here, we report rate constants of the CN + benzene (C_6H_6) and CN + toluene (C_7H_8) reactions between 15 and 294 K using a CRESU apparatus coupled with the pulsed laser photolysis – laser induced fluorescence (PLP-LIF) technique. We also present the stationary points on the CN + toluene potential energy surface of this reaction to study the available reaction pathways. We find that both rate constants do not change over this temperature range, with an average value of $(4.4 \pm 0.2) \times 10^{-10}$ cm^3 s^{-1} for the CN + benzene reaction, in good agreement with previous measurements, and $(4.1 \pm 0.2) \times 10^{-10}$ cm^3 s^{-1} for the CN + toluene reaction, which is notably faster than the only previous measurement at 105 K. While the reason for this disagreement is unknown, we discuss the possibility that it is related to enhanced multiphoton effects in the previous work.

4.2 – Introduction

The CN radical has long been known to be abundant in the interstellar medium (ISM), where it was first detected in 1940s,[1-2] and in the atmosphere of Titan, where it leads the formation of nitrile compounds, including C_2H_3CN and HC_3N.[3-5] At the low temperatures found in these environments, reactions between CN and other compounds are known to have fast rate constants, on the order of 10^{-10} cm^3 s^{-1}, and thus must be included in gas-phase models. Reactions between CN and hydrocarbons are among the fastest of these rates, and proceed through either an abstraction or an addition mechanism.[6] A number of cyano-containing molecules linked to these reactions have been found in ISM, including molecules as large as HC_9N[7] and $(CH_3)_2CHCN$.[8] On Titan, the photolysis of these nitrile compounds formed from CN reactions may contribute to the formation of particulate matter.[9]

On Titan, both benzene and toluene have been detected in the upper atmosphere by the Cassini Ion and Neutral Mass Spectrometer,[10-11] and while currently undetected in the lower atmosphere, models suggest both have high abundances there as a product of the fast association reactions between C_6H_5 and H or CH_3.[12] In addition to benzene and toluene, a large number of specific polycyclic aromatic hydrocarbons (PAHs) have also been identified.[13] These PAHs are believed to form from smaller aromatic compounds and to be an important component of the thick haze in Titan's atmosphere.[14]

On the other hand, very few specific aromatic molecules have been directly detected in the ISM, in part due to their low dipole moments making them unable to be observed by radio astronomy. Benzene has been observed through observations of weak infrared transitions,[15] and PAHs are widely believed to be abundant in the ISM owing to

observations of the strong infrared bands characteristic of these molecules, but the broad, overlapping nature of these bands has precluded the identification of specific PAHs.[16] Despite this lack of definitive identifications, PAHs are believed to hold a large fraction of carbon in the ISM,[17-18] and so their formation has been the subject of extensive study.[19-21] The formation of the first aromatic ring is believed to be the rate limiting step in PAH formation,[22] and so understanding the chemistry of these monocyclic aromatic compounds is necessary.

The recent detection of benzonitrile in the ISM[23] has suggested a new route for understanding aromatic formation. Benzonitrile is believed to be the product from the CN + benzene reaction. Observations of benzonitrile therefore can be used as a proxy for the abundance of benzene. Other aromatic nitriles may also serve as proxies for undetected aromatic compounds in the ISM, as the addition of the cyano moiety gives these compounds large dipole moments and makes them visible to radio astronomy. The identification of additional specific aromatic compounds would significantly constrain models of PAH formation in the ISM.

However, little is known about the rates and products of the reactions of CN with aromatic molecules. The only previous measurements come from Trevitt et al.[24], who studied the CN + benzene reaction at 105, 165 and 29 K, and the CN + toluene reaction at 106 K, using pulsed laser photolysis – laser induced fluorescence (PLP-LIF) measurements in conjunction with a pulsed Laval nozzle. For the benzene reaction, they found a rate of $(3.9 – 4.9) \times 10^{-10}$ cm^3 s^{-1}, with no change as function of temperature, and for the toluene reaction, they determined a rate constant of $(1.3 \pm 0.3) \times 10^{-10}$ cm^3 s^{-1}. The fact that the rate constant of the CN + toluene reaction is a factor of 3 lower than the rate constants measured

for the CN + benzene reaction suggest that the structure of aromatic molecules can play a large role in the reaction rates. Furthermore, they observed non-exponential decays of CN at room temperature in the presence of toluene and were therefore unable to measure a rate constant, in contrast with their measurements of benzene under the same conditions. They suggested that this could be due to dissociation of the products back to the CN + toluene reactants, and that further studies would be necessary to better understand these results.

The lack of experimental rate constants for the CN + benzene reaction at temperatures relevant to the interstellar medium would improve our understanding of this reaction and determine whether it may be the pathway that forms benzonitrile in the ISM. Furthermore, the difference between the rate constants of the CN + benzene and CN + toluene reactions suggests that the structure of an aromatic compound can play a large role in the reaction dynamics. This makes it questionable whether nitrile compounds may be formed from the reactions of CN with larger, more complex aromatic compounds, and it is essential to verify the reliability of using cyano-substituted compounds as a proxy for larger aromatic species. To these ends, we have conducted measurements of the CN + benzene and CN + toluene rate constants between 15 and 294 K to gain further insight into these reactions, especially at the low temperatures relevant to the ISM and Titan. Furthermore, we have computed stationary points on the potential energy surface (PES) of the CN + toluene reaction, which have not been previously determined, to better understand the possible products and mechanism of this reaction.

4.3 – Experimental Methods

Rate constants were determined using the PLP-LIF technique. Temperatures down to 15 K were achieved using the CRESU technique which has been described in detail

previously[6, 25-26] and in Chapter 2. Briefly, benzene (Sigma Aldrich, anhydrous 99.8%) or toluene (Sigma Aldrich, 99.9%) were introduced into the gas flow with a Controlled Evaporation and Mixing system (Bronkhorst CEM), as described in Gupta et al.[27] The benzene/toluene and ICN (Acros Organics, 98%), used as the CN precursor, were mixed in a buffer gas of He (99.995%, Air Liquide), Ar (99.998%, Air Liquide) or N_2 (99.995%, Air Liquide), depending on the desired CRESU conditions. Concentrations of benzene/toluene and ICN were kept < 1% of the total density in order not to affect the uniformity of the gas flow. The mixture was flowed isentropically from a high-pressure reservoir through specifically designed convergent-divergent Laval nozzles, into a low-pressure chamber to generate a uniform supersonic flow at the appropriate temperature with a density of $10^{16} – 10^{17}$ cm^{-3}. Each nozzle was characterized with Pitot probe impact pressure measurements prior to experiments to determine the temperature, density and uniformity of the gas flow. For measurements at 294 K, where a supersonic expansion is not required, the pumping speed was decreased such that the pressure in the reservoir and the chamber were equal, while maintaining complete gas turnover for each laser shot.

As detailed in Chapter 2, CN radicals were generated by the 248 nm photolysis of ICN using a KrF excimer laser operating at 10 Hz, with a laser fluence of 25 mJ cm^{-2}. The third harmonic of a Nd:YAG laser, also operating at 10 Hz, was used to pump a dye laser containing Exalite 389 in 1,4-dioxane to produce ~389 nm light to excite the CN $B^2\Sigma^+$ - $X^2\Sigma^+$ (0,0) transition. Fluorescence was detected from the CN (0,1) transition at ~420 nm by a photomultiplier tube preceded by a 420 nm bandpass filter. The delay time between the excimer and the Nd:YAG pump laser was varied from -5 to 200 microseconds to record the time dependence of the CN signal. The LIF signal was recorded by a gated integrator

at 400 evenly spaced points and averaged 5 times. The resulting kinetic trace was fit to an exponential decay starting ≥ 10 μs after photolysis to allow for rotational thermalization of CN.

Kinetic measurements were taken under pseudo-first order conditions with [aromatic] >> [CN]. Typical benzene and toluene concentrations were on the order of 10^{12} – 10^{13} cm^{-3}, while we estimate the CN concentration to be roughly 10^{10} cm^{-3} based on the ICN concentration (~10^{12} cm^{-3}) and 248 nm absorption cross section of 4.7×10^{-19} cm^2.[28] More than 90% of the CN radicals from the photolysis of ICN at 248 nm are in the ground vibrational state[29] and we do not observe any influence of the relaxation of excited vibrational states on our kinetic measurements.

4.4 – Computational Methods

Investigation of possible channels for the reaction between CN and toluene, with identification of all the stationary points (minima, complexes, and transition states), was done by Divita Gupta using Gaussian 09 software[30]; all included channels can be seen in Figure 4.1. All the species, including the reaction complexes and transition states were optimized at (U)M06-2X/aug-cc-pVTZ level[31-33] and zero-point corrected energies were calculated for each. In addition, intrinsic reaction coordinate (IRC) calculations were performed at (U)M06-2X/6-311G to determine the minimum energy path that the transition states followed to confirm the connection between the appropriate reactants and products. Gibbs energies ($\Delta_r G^o$ 298 K) at 298 K for all included channels were also calculated at (U)M06-2X/aug-cc-pVTZ method. Both addition-elimination channels, leading to nitrile formation, and abstraction channels, leading to HCN formation, are considered. While reactions involving the CN radical may produce both cyano and isocyano compounds, only

the former pathways are considered in these calculations. Previous work on the CN + benzene reaction[34] showed a significant barrier (28 kJ mol^{-1}) to isocyano products, which suggests that this pathway will not be relevant in the ISM.

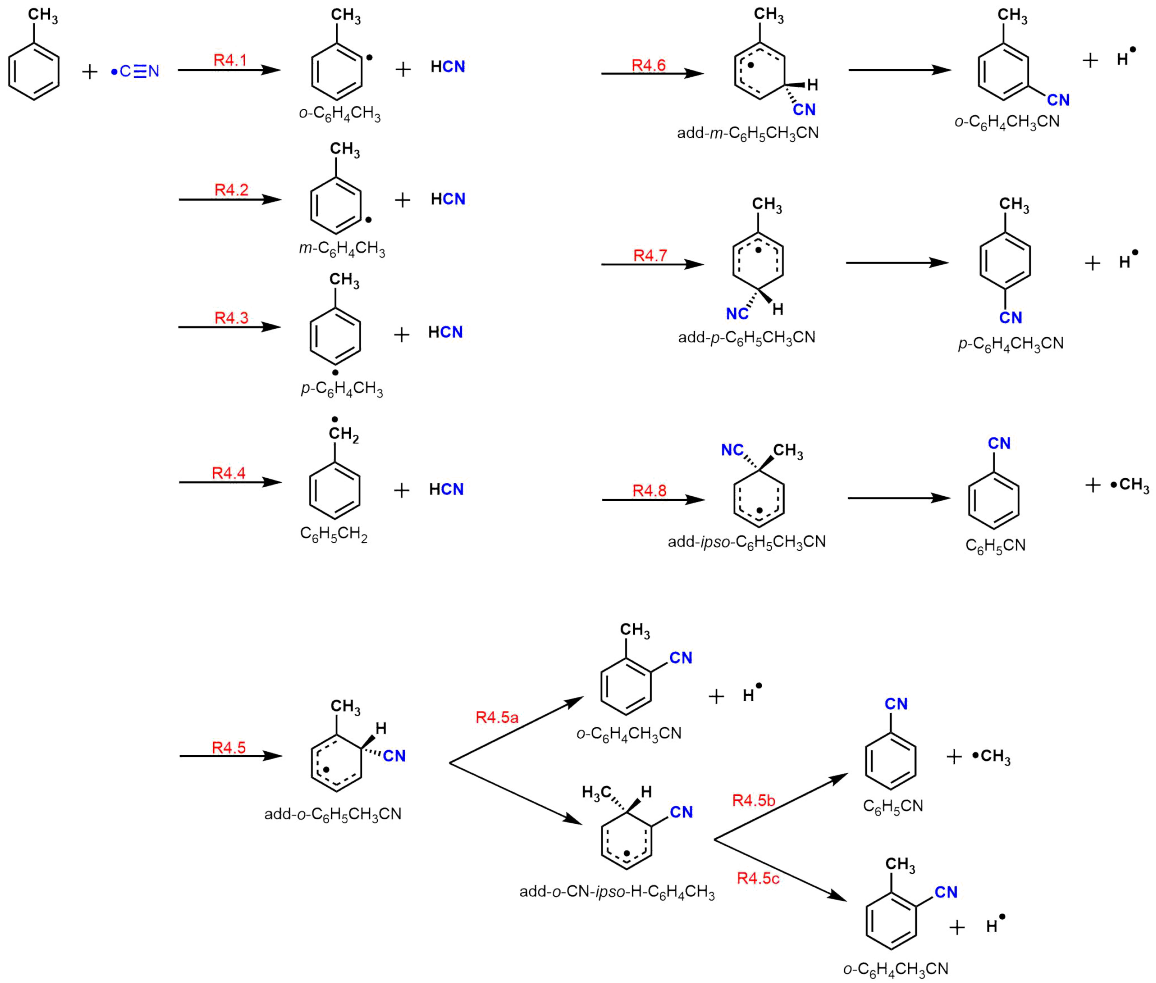

Figure 4.1: The reaction pathways of the CN + toluene reaction and possible products of the abstraction (R4.1-R4.4) and CN-addition (R4.5-R4.8) channels that are considered in the theoretical calculations.

4.5 – Results

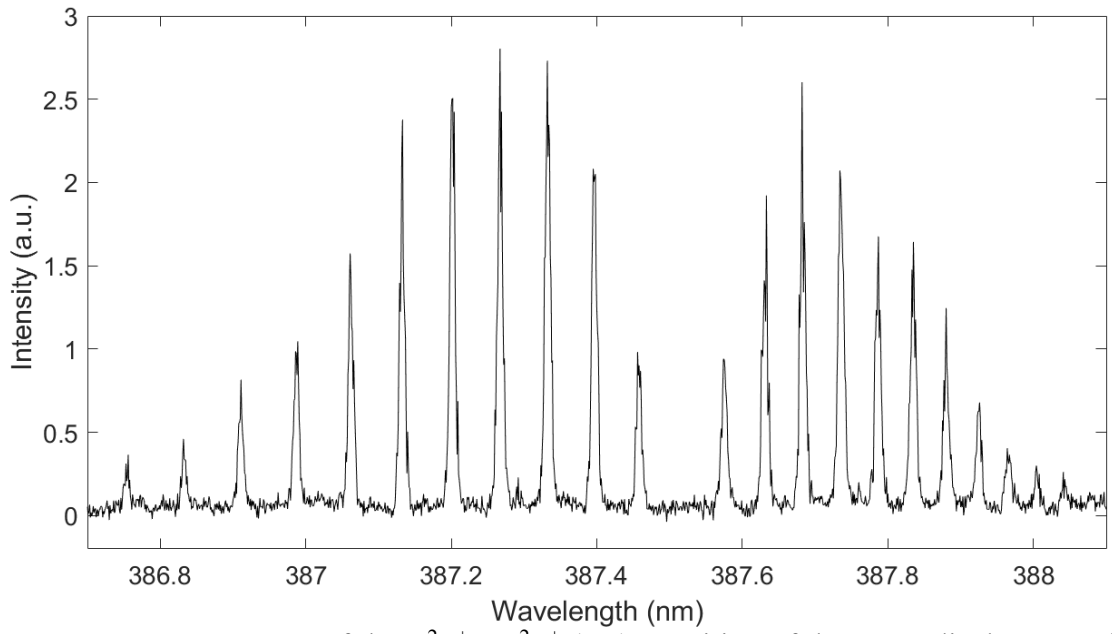

Figure 4.2: LIF spectrum of the $B^2\Sigma^+$ - $X^2\Sigma^+$ (0,0) transition of the CN radical at 72 K in He.

An experimental spectrum of the CN $B^2\Sigma^+$ - $X^2\Sigma^+$ (0,0) spectrum at 72 K can be seen in Figure 4.2. As the temperature decreases, fewer rotational states of CN have significant populations and therefore fewer transitions are observed. Typical LIF decays of CN from the CN + toluene reaction at 83 K and 294 K and the second-order plots can be seen in Figures 4.3 and 4.4, respectively. The non-zero intercepts seen on the second-order plots arise from the loss of CN via side chemistry and diffusion out of the region probed by LIF. From experiments at room temperature, using He and N_2 as the buffer gases, and varying the total density of the gas flow, we found that the rate constants for both reactions have no pressure dependence, implying that the reactions are either bimolecular reactions, or termolecular reactions in the high pressure limit in our experimental conditions. Unlike the room temperature measurements of the CN + toluene reaction by Trevitt et al., we see no evidence for non-exponential decays at any toluene concentration or total gas density

used in these experiments, and the measured rate constants are in good agreement with our values at all other temperatures.

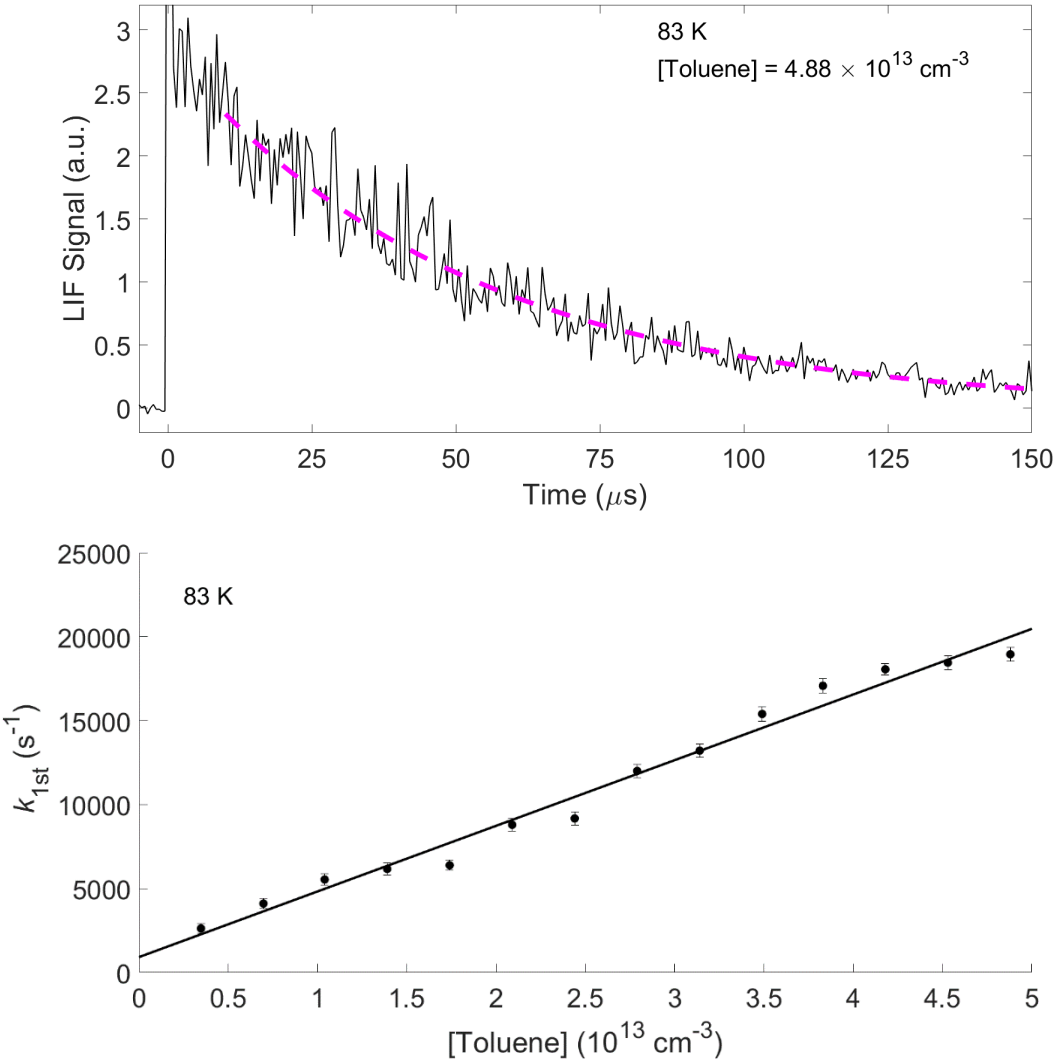

Figure 4.3: Typical experimental kinetics of the CN + toluene reaction measured using PLP-LIF, showing the decay of the CN signal (top) and resulting second-order plot at 83 K (bottom).

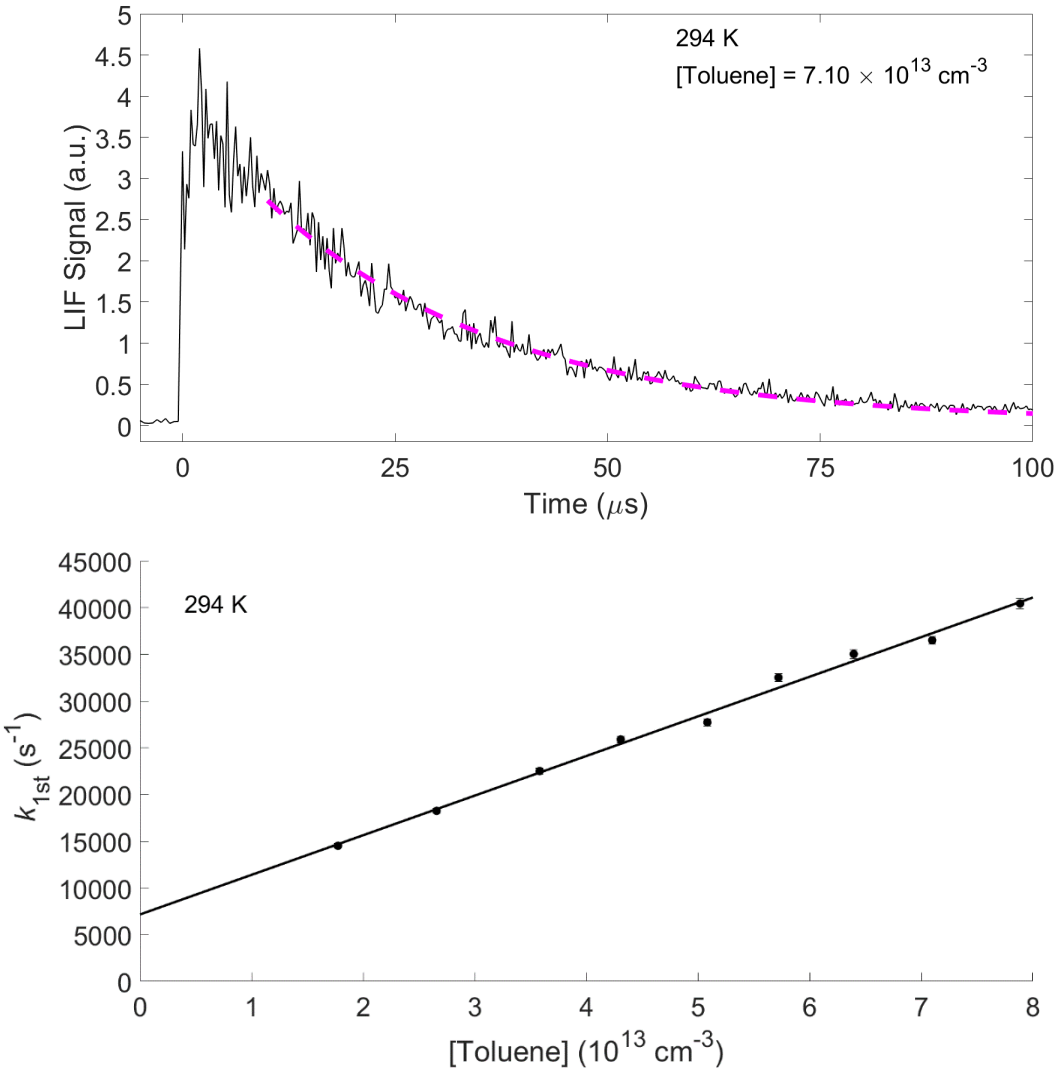

Figure 4.4: Typical experimental kinetics of the CN + toluene reaction measured using PLP-LIF, showing the decay of the CN signal (top) and resulting second-order plot at 294 K (bottom).

Results of the experiments between 15 and 294 K are shown in Table 4.1 and Figure 4.5 for the CN + benzene reaction, and Table 4.2 and Figure 4.6 for the CN + toluene reaction. At least eight points with varying benzene/toluene concentrations were taken for each measurement under pseudo-first order conditions, with the aromatic molecule in excess. At high aromatic concentrations, the formation of benzene or toluene dimers causes nonlinear behavior in the second-order plots at the lowest temperatures. This therefore

imposes an upper limit on the benzene and toluene concentrations used in experiments in order to minimize any effect of the reaction between CN and aromatic dimers on our measurements.

Table 4.1: Rate coefficients determined for the CN + benzene reaction between 15 and 294 K, along with experimental parameters for each measurement. Uncertainties in the rate constant are the 95% confidence interval from the appropriate Student's *t* test combined in quadrature with a 10% systematic error. Bolded values represent the weighted average and uncertainty for temperatures with multiple measurements.

Temperature (K)	Buffer Gas	Total Density (10^{16} cm^{-3})	[Benzene] (10^{12} cm^{-3})	Number of Points	Rate Constant (10^{-10} cm^3 s^{-1})
15	He	5.02	2.19 – 19.7	13	5.5 ± 0.9
15	He	5.02	2.19 – 17.5	14	5.4 ± 0.9
					5.4 ± 0.6
17	He	4.85	2.03 – 14.2	13	4.5 ± 0.7
24	He	4.85	2.08 – 22.8	11	5.1 ± 0.7
36	He	5.31	1.48 – 14.8	11	5.4 ± 0.7
36	He	5.27	1.47 – 20.6	14	5.5 ± 0.9
36	He	5.27	1.47 – 14.7	11	5.2 ± 0.8
					5.3 ± 0.6
72	He	6.01	1.54 – 24.6	14	5.5 ± 0.6
72	He	6.01	3.00 – 16.5	12	5.1 ± 0.7
					5.4 ± 0.6
83	N_2	4.61	2.06 – 16.5	8	3.9 ± 0.7
83	N_2	4.61	2.04 – 24.6	12	3.9 ± 0.6
					3.9 ± 0.4
110	Ar	2.71	1.66 – 19.9	11	4.2 ± 0.6
200	N_2	5.27	2.52 – 20.2	13	3.7 ± 0.8
294	N_2	7.04	1.52 – 76.1	9	3.5 ± 0.4
293	N_2	9.78	1.53 – 76.6	9	3.5 ± 0.4
293	N_2	18.5	2.21 – 69.6	8	3.3 ± 0.5
293	He	5.27	6.25 – 37.5	9	4.0 ± 0.6
293	He	6.92	2.03 – 81.3	10	3.4 ± 0.5
293	He	9.39	2.16 – 63.4	6	4.1 ± 0.6
295	He	9.10	1.50 – 74.8	9	4.0 ± 0.5
					3.6 ± 0.4

Table 4.2: Rate coefficients determined for the CN + toluene reaction between 15 and 294 K, along with experimental parameters for each measurement. Uncertainties in the rate constant are the 95% confidence interval from the appropriate Student's *t* test combined in quadrature with a 10% systematic error. Bolded values represent the weighted average and uncertainty for temperatures with multiple measurements.

Temperature (K)	Buffer Gas	Total Density (10^{16} cm^{-3})	[Toluene] (10^{12} cm^{-3})	Number of Points	Rate Constant (10^{-10} cm^3 s^{-1})
15	He	5.04	1.87 – 10.4	10	4.4 ± 0.8
24	He	4.83	1.76 – 19.5	11	4.7 ± 0.6
36	He	5.27	1.25 – 17.7	14	5.9 ± 0.8
36	He	5.32	1.28 – 12.7	9	4.9 ± 1.0
					5.7 ± 0.7
70	He	6.00	2.54 – 15.2	11	4.4 ± 0.7
70	He	6.09	1.34 – 18.7	13	4.2 ± 0.7
					4.3 ± 0.6
83	N_2	4.63	3.48 – 48.8	14	3.9 ± 0.5
83	N_2	4.63	1.72 – 31.3	14	3.8 ± 0.4
					3.9 ± 0.4
110	Ar	2.71	1.28 – 14.1	11	3.3 ± 0.5
197	N_2	5.32	2.13 – 21.4	11	3.7 ± 0.6
294	N_2	10.5	15.4 – 92.9	11	3.7 ± 0.6
294	N_2	3.75	9.50 – 47.6	9	4.3 ± 0.6
294	N_2	8.20	17.7 – 78.9	9	4.3 ± 0.5
294	He	9.41	18.0 – 54.0	11	4.5 ± 0.5
					4.3 ± 0.5

To test whether the photolysis of benzene or toluene at 248 nm affected our measurements, we also conducted experiments varying the power of the excimer laser, by determining whether the decay of the CN radical changed as a function of excimer power. The benzene experiments were conducted at 24 K and [benzene] = 2×10^{12} cm^{-3}, and the toluene experiments were conducted at 110 K, with [toluene] = 9×10^{12} cm^{-3}. We found no significant change in the measured k_{1st} as a function of our laser power for either. With the excimer laser fluence of 25 mJ cm^{-2} and the absorption cross sections at 248 nm (1.4×10^{-19} cm^2 for benzene[35] and 2.9×10^{-19} cm^2 for toluene[36]) we expect roughly 1% of the aromatic compounds to photolyze if the photolysis quantum yield is 1, which should not

measurably affect the observed rate constants. However, it has been suggested that photolysis does not occur after single photon absorption at 248 nm, only two-photon absorption, which can photolyze the aromatics to form H atoms among other potential processes.[37] The total absorption cross section for the second photon experimentally determined to be 2.8×10^{-17} cm^2 for benzene and 1.7×10^{-17} cm^2 for toluene.[37] For the highest aromatic concentrations used (~1×10^{14} cm^{-3}), we estimate at most 4.8×10^{11} cm^{-3} of benzene or toluene undergoes two-photon absorption, though it is likely much less than that, as discussed in greater detail in the following section in the case of toluene, and is unlikely to affect the rate constants measured.

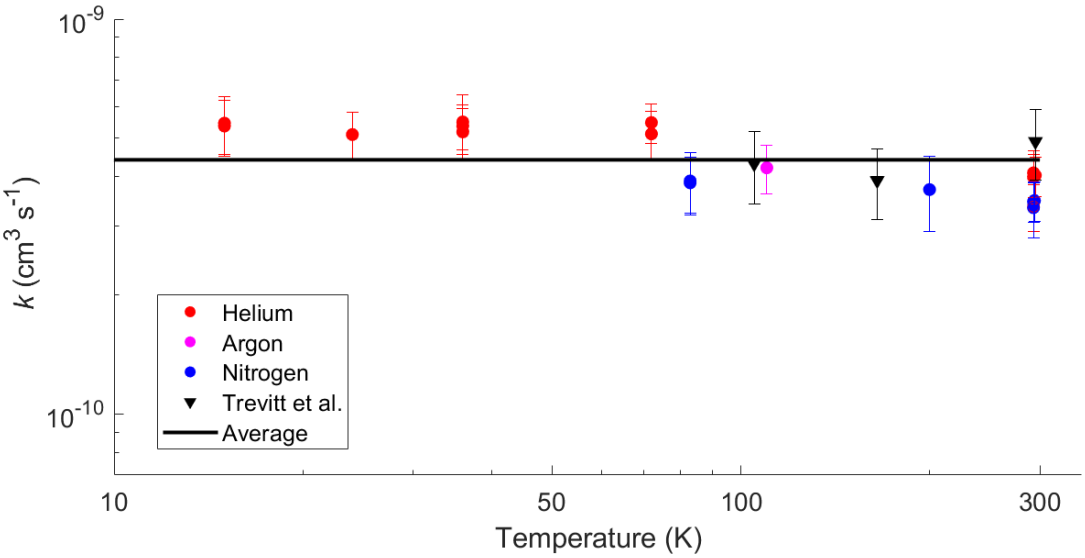

Figure 4.5: The experimental measurements for the CN + benzene rate constant from this work (circles) and Trevitt et al. (triangles); the weighted average value of the measurements presented in this work, 4.4×10^{-10} cm^3 s^{-1}, is also plotted.

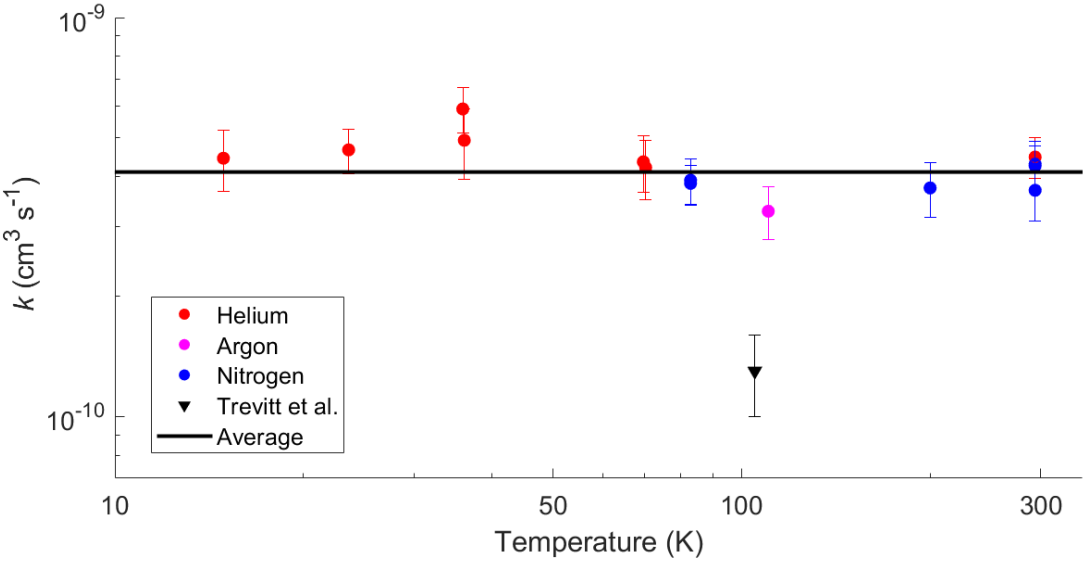

Figure 4.6: The experimental measurements for the CN + toluene rate constant from this work (circles) and Trevitt et al. (triangle); the weighted average value of the measurements presented in this work, 4.1×10^{-10} cm^3 s^{-1}, is also plotted.

Table 4.3: Zero-point corrected reaction energies and Gibbs energies of the CN + toluene reaction products calculated in this work. Note that some reaction pathways result in the same products.

Reaction channel products	Reaction energy $\Delta_r U^o$ (kcal mol^{-1})	Gibbs energy $\Delta_r G^o$ (298 K) (kcal mol^{-1})
R4.1 (*o*-$C_6H_4CH_3$ + HCN)	-18.1	-18.1
R4.2 (*m*-$C_6H_4CH_3$ + HCN)	-18.3	-18.6
R4.3 (*p*-$C_6H_4CH_3$ + HCN)	-17.8	-18.2
R4.4 ($C_6H_5CH_2$ + HCN)	-39.1	-38.1
R4.5a (= R5c, *o*-$C_6H_4CH_3CN$ + H)	-28.0	-23.6
R4.5b (= R8, C_6H_5CN + CH_3)	-35.4	-35.5
R4.5c (= R5a, *o*-$C_6H_4CH_3CN$ + H)	-28.0	-23.6
R4.6 (*m*-$C_6H_4CH_3CN$ + H)	-26.8	-22.5
R4.7 (*p*-$C_6H_4CH_3CN$ + H)	-27.2	-23.8
R4.8 (= R5b, C_6H_5CN + CH_3)	-35.4	-35.5

As shown in the Figure 4.7, both stationary points (reactants, products, intermediates, transition states) for both the abstraction (R4.1-R4.4) and addition-elimination (R4.5-R4.8) channels were characterized for the reaction between CN and toluene. An additional substitution channel, leading to the formation of benzyl cyanide,

was found to be exothermic at (U)M06-2X/aug-cc-pVTZ, but has a large barrier (~20 kcal mol^{-1}), and hence will not be relevant under interstellar conditions and is excluded. The relative reaction energy $\Delta_r U^o$ and Gibbs energy at 298 K $\Delta_r G^o$ for all calculated product channels can be seen in Table 4.2. Intermediates formed from the addition of CN to the aromatic ring were found to form barrierlessly, subsequently followed by submerged barriers leading to the formation of stable nitrile products. This mechanism closely resembles the mechanism of benzonitrile formation from the reaction of benzene and CN,[34,38] although it does differ from the reaction between toluene and OH, which features both pre-reactive complexes and barriers before formation of the addition product.[39] The energies determined for the addition-elimination channels are generally similar to those calculated for the CN + benzene reaction done at G3//B3LYP and BCCSD(T)//B3LYP.[34]

Abstraction pathways, shown in blue in Figure 4.5, were found to have slightly submerged transition states, and therefore are possible products at low temperatures. However, higher level calculations are needed to confirm these barrier values, as similar abstraction pathways from aromatic compounds have been shown to possess positive barriers[38-39]. At the level of theory used, these barrier values are likely within the error of the calculations. An important point to note is that no transition state or complex could be characterized for the abstraction channels, though we do not rule out the existence of these stationary points.

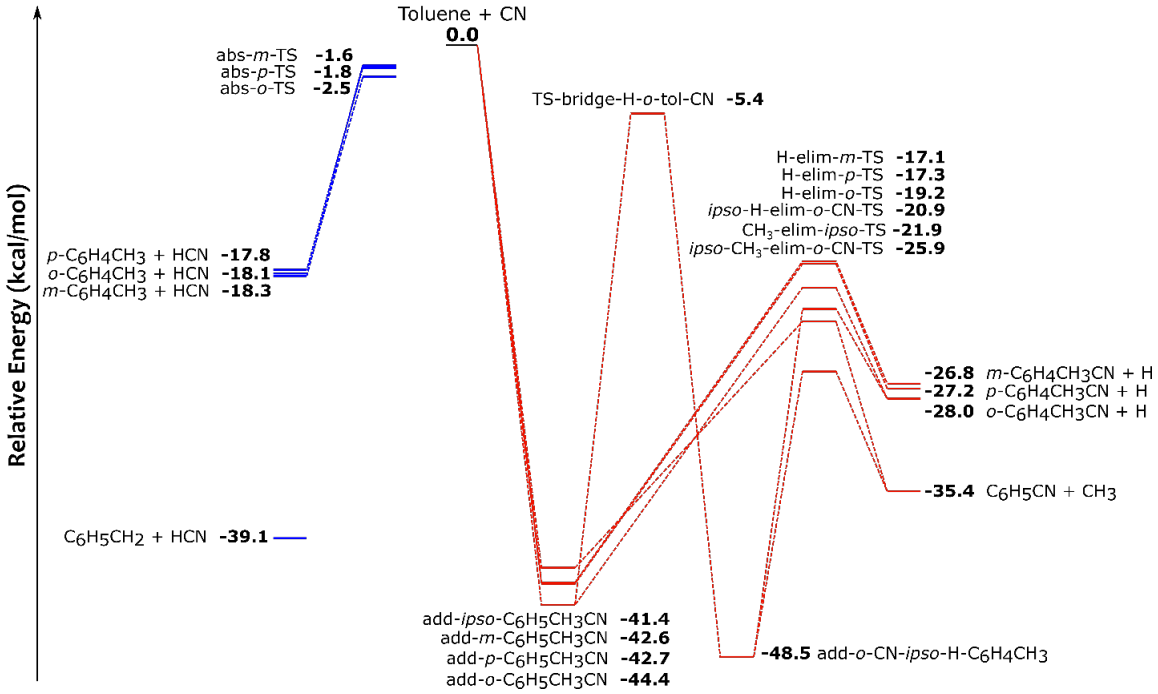

Figure 4.7: The stationary points for PES for the CN + toluene reaction, performed at (U)M06-2X/aug-cc-pVTZ including zero-point energy corrections. Both the abstraction (abs-) pathways (blue) and addition-elimination (add- and elim-) pathways (red) are shown, the latter of which can undergo an internal hydrogen shift (-bridge). Note that neither a barrier leading to the formation of $C_6H_5CH_2$ + HCN nor any pre-reactive complexes for the abstraction pathways are included, though we do not preclude their existence.

4.6 – Discussion

As Figures 4.5 and 4.6 demonstrate, we find that the rate constant of both the CN + benzene reaction and the CN + toluene reactions are independent of temperature over the 15 – 294 K range. We find that the CN + benzene reaction rate constant has a weighted average value of $(4.4 \pm 0.2) \times 10^{-10}$ cm^3 s^{-1} , while the CN + toluene reaction rate constant has a weighted average value of $(4.1 \pm 0.2) \times 10^{-10}$ cm^3 s^{-1}. Our results for the CN + benzene reaction are in good agreement the results of Trevitt et al., but there is a notable discrepancy when comparing our CN + toluene results, as they measured a rate constant of $(1.3 \pm 0.3) \times 10^{-10}$ cm^3 s^{-1} for that reaction at 106 K in their LIF experiments. They used a similar LIF method to detect CN, under similar experimental conditions of total density, and CN and

toluene concentrations. Furthermore, the agreement our respective CN + benzene rate constants suggests that this discrepancy is related somehow to the toluene system.

Trevitt et al. reported observing non-exponential decays of CN at room temperature, which they suggested might be due to back-dissociation of adduct complexes. However, no such behavior was observed in this work, suggesting that the discrepancy might have arisen from differences in the photolysis step. Trevitt et al. photolyzed their sample at a wavelength of 266 nm, with a laser fluence of 40 mJ cm^{-2} (5.0×10^{16} photons cm^{-2}, in a probable 3-5 ns long pulse), in contrast to the 248 nm laser beam with a fluence of 25 mJ cm^{-2} (3.1×10^{16} photons cm^{-2}, 22 ns long pulse) used in this work. The ICN photolysis cross sections are similar at these two wavelengths.[28, 40] At room temperature, the toluene absorption cross section to the S_1 state at 266 nm is 1.3×10^{-19} cm^2.[41] The S_1 state fluoresces with a lifetime of 86 ns when excited at 266 nm at low pressures.[42] At 248 nm, the cross section is larger (2.9×10^{-19} cm^2)[41] but the fluorescence lifetime is much shorter due to rapid internal conversion to S_0, displaying approximately equal intensity 3 ns and 26 ns components at low pressures.[43] As discussed above, multiphoton absorption at 248 nm of toluene is known to lead to photolysis,[37] and may additionally lead to photoionization, as the excited toluene is higher in energy than the ionization onset of toluene (8.3 eV).[44] Both of these processes are also likely to occur in the 266 nm experiments.

The above considerations suggest that single photon excitation of toluene is occurring at both photolysis wavelengths, but only multiphoton effects are likely to give rise to interferences. Possible pathways for CN generation on the timescale of the experiment exist by either two-photon photodissociation or two-photon ionization,

particularly at 266 nm by quadrupled Nd:YAG lasers. Such effects are likely to be significantly lower when toluene is excited at 248 nm light produced by an excimer, due to the longer pulse duration and rapid internal conversion of the S_1 state. This is in good agreement with the experimental measurements reported here, showing no relationship between excimer power and k_{1st}, and no evidence for non-exponential decays. In the experiments of Trevitt et al. at 266 nm, however, the long lifetime of the S_1 state, short photolysis pulse duration and higher laser fluence may have caused larger amounts of multi-photon absorption to occur, such that photodissociation or photoionization products could have affected their measurements.

Further work from Trevitt et al. measured the products of the CN + benzene and CN + toluene reactions at room temperature, using slow flow reactors in conjunction with product detection by multiplexed photoionization mass spectrometry (MPIMS) to identify species by mass and photoionization spectrum. They found that the reaction between CN and benzene exclusively forms benzonitrile, while the CN and toluene exclusively forms tolunitrile (methylbenzonitrile), with no evidence for the hydrogen abstraction channels or methyl-loss channels. Due to the similarities in the calculated photoionization spectra of the *ortho*, *meta*, and *para* isomers of the tolunitrile, they were unable to distinguish the precise isomers of tolunitrile formed from CN + toluene. Lenis and Miller also measured the products of the CN + toluene reaction using the 254 nm photolysis of ICN and analyzing the resulting products with GC-MS[45] and observed both tolunitrile and a small yield (9%) of benzonitrile. While it is unclear if this benzonitrile is formed as a result of CN + toluene or side chemistry, particularly in light of its non-detection in the MPIMS

experiments by Trevitt et al., our calculations do show potential pathways to benzonitrile formation from *ortho* or *ipso* addition of CN to the aromatic ring.

The rate constants measured here for the CN + benzene and the CN + toluene systems are in good agreement with each other. In conjunction with the similarities in products measured by MPIMS, this suggests that the major mechanism is the same for reactions between the CN radical and either benzene or toluene, and results in formation of cyano-substituted aromatic compounds. Investigation of other substituted compounds, such as xylenes or deuterium-substituted benzene, may yield further insight into whether this mechanism is general for these reactions. This will aid in future astronomical searches to improve our understanding of the formation of small aromatic rings in the ISM.

The submerged barriers found for the various channels of the CN + toluene reaction using quantum chemical calculations highlight the diversity of the products that could be formed from this reaction at low temperatures. While the abstraction channels were found to have slightly submerged barriers, calculations at higher level of theory are necessary to correctly estimate their energies. Furthermore, the transition state(s) and/or a possible complex in the case of the hydrogen abstraction from the methyl group pathway remain to be explored further. This will also provide the accuracy necessary for master equation calculations, which would further elucidate the mechanism and product branching ratios of this reaction.

On Titan, the CN radical is mainly generated from the photolysis of HCN, which is formed through reactions of $N(^4S)$ or through ion chemistry.[4-5] Once formed, CN reacts primarily with the highly abundant CH_4 to reform HCN. This cycle can be interrupted, however, by CN reactions with other compounds, most commonly C_2H_2 or HC_3N. While

this reaction has not explicitly been included in models, recent work has suggested that the concentrations of benzene and toluene in the Titan atmosphere are similar, peaking at a mole fraction of 10^{-6} at an altitude of roughly 1000 km above the surface.[12] Benzonitrile has not been detected on Titan and is predicted to be formed in low quantities, largely due to CN being sequestered by reaction with CH_4. Even with the larger rate constants measured in this work, this is likely also the case for the products of the reaction between CN and toluene, though implementation of these results into Titan models may still be beneficial to determine if they have any influence in the atmosphere.

Astronomical searches for toluene and the tolunitrile products of this reaction would test the robustness of using cyano-containing species as proxies for the unsubstituted hydrocarbons. While benzene has no permanent dipole moment, toluene has a small one (0.37 Debye)[46] and may be observable via radio astronomy, thought it would have to be present in higher abundance than molecules with large dipole moments, like benzonitrile, to be detectable. The use of velocity stacking, which averages the signal of multiple transitions together to increase the signal-to-noise ratio,[47-49] may assist in searching for toluene in the ISM. While there have been no previous detections of toluene in the ISM, it has been argued that the protonated toluene ion, $C_7H_9^+$,[50] and methyl-substituted PAHs[51-52] are possible carriers of the 6.2 and the 3.4 μm unidentified infrared bands, respectively. Definitive detection of toluene and related compounds, such as these, would allow us to constrain aromatic pathways and, in particular, could test the bottom-up mechanism for PAH formation, wherein small molecules, such as toluene, react progressively to form large clusters.

The origin of the first aromatic ring in the interstellar medium in molecules such as benzene and toluene remains unknown. It has been argued that the reaction between C_2H and the unsaturated hydrocarbons 1,3-butadiene and isoprene (C_5H_8; 2-methyl-1,3-butadiene), which are barrierless reactions that produce benzene and toluene, respectively, may be a source of them at low temperatures.[53-54] However, neither 1,3-butadiene nor isoprene have been detected in the ISM. Isoprene is also not included in astrochemical databases such as the Kinetic Database for Astrochemistry[55] (kida.obs.u-bordeaux1.fr, accessed July 2020). Other mechanisms, such as ion-neutral reactions, may also contribute, but further investigation is necessary. The reaction of C_2H and 1,3-butadiene has been used in astrochemical models of the ISM to explain benzene formation,[23] but there is debate as to how much benzene is actually formed from this reaction, as it has been shown that fulvene is the major product.[56]

In order to better understand the potential formation pathways of these products of the CN + toluene in the ISM, more accurate measurements of the product ratios are required, and specifically, the branching ratio for the tolunitrile and potential benzonitrile products. While challenging for many techniques due to the similarities of the isomers, recent work has coupled low temperature supersonic uniform flows to microwave spectrometers[57-58] in order to determine branching ratios relevant for astrochemistry. As each of these compounds will have a unique rotational spectrum, this technique is well suited for quantitatively measuring the product branching ratio of this reaction. Low temperature product measurements of the CN + benzene reaction would also provide further evidence that this reaction is responsible for the formation of benzonitrile in ISM.

4.7 – Conclusions

We have measured rate constants for the CN + benzene and CN + toluene reactions between 15 and 294 K, and find that these rate constants are independent of temperature over this range. These results closely match the previous measurements down to 105 K for the CN + benzene reaction, but are a factor of three higher than the only previous measurement of CN + toluene rate constant at 105 K. The reasons for this discrepancy remain unresolved, but may be related to multiphoton effects at the higher laser intensities and 266 nm photolysis wavelength used in that study. This similarly suggests that the reactions between CN and simple aromatics proceed through an analogous mechanism, which is supported by our theoretical calculations and previous product measurements. Further work, particularly on the products formed from the CN + toluene, would be beneficial to determine their potential detectability in the ISM. The ability to detect and use cyano-substituted aromatics, which have large dipole moments, as proxies for unsubstituted aromatic compounds in the ISM would help advance our knowledge of PAH formation.

4.8 – References

1. Adams, W. S., Some Results with the Coude Spectrograph of the Mount Wilson Observatory. *Astrophys J* **1941**, *93*, 11-23.

2. McKellar, A., Evidence for the Molecular Origin of Some Hitherto Unidentified Interstellar Lines. *Publ Astron Soc Pac* **1940**, *52*, 187 - 192.

3. Yung, Y. L.; Allen, M.; Pinto, J. P., Photochemistry of the Atmosphere of Titan - Comparison between Model and Observations. *Astrophys J Suppl S* **1984**, *55*, 465-506.

4. Loison, J. C.; Hebrard, E.; Dobrijevic, M.; Hickson, K. M.; Caralp, F.; Hue, V.; Gronoff, G.; Venot, O.; Benilan, Y., The Neutral Photochemistry of Nitriles, Amines and Imines in the Atmosphere of Titan. *Icarus* **2015**, *247*, 218-247.

5. Wilson, E. H.; Atreya, S. K., Current State of Modeling the Photochemistry of Titan's Mutually Dependent Atmosphere and Ionosphere. *J Geophys Res* **2004**, *109*, E06002.

6. Cooke, I. R.; Sims, I. R., Experimental Studies of Gas-Phase Reactivity in Relation to Complex Organic Molecules in Star-Forming Regions. *ACS Earth Space Chem* **2019**, *3*, 1109-1134.

7. Broten, N. W.; Oka, T.; Avery, L. W.; Macleod, J. M.; Kroto, H. W., The Detection of HC_9N in Interstellar Space. *Astrophys J* **1978**, *223*, L105-L107.

8. Belloche, A.; Garrod, R. T.; Muller, H. S. P.; Menten, K. M., Detection of a Branched Alkyl Molecule in the Interstellar Medium: Iso-Propyl Cyanide. *Science* **2014**, *345*, 1584-1587.

9. Gudipati, M. S.; Jacovi, R.; Couturier-Tamburelli, I.; Lignell, A.; Allen, M., Photochemical Activity of Titan's Low-Altitude Condensed Haze. *Nat Commun* **2013**, *4*, 1648.

10. Magee, B. A.; Waite, J. H.; Mandt, K. E.; Westlake, J.; Bell, J.; Gell, D. A., INMS-Derived Composition of Titan's Upper Atmosphere: Analysis Methods and Model Comparison. *Planet Space Sci* **2009**, *57*, 1895-1916.

11. Vuitton, V.; Yelle, R. V.; Cui, J., Formation and Distribution of Benzene on Titan. *J Geophys Res-Planet* **2008**, *113*.

12. Loison, J. C.; Dobrijevic, M.; Hickson, K. M., The Photochemical Production of Aromatics in the Atmosphere of Titan. *Icarus* **2019**, *329*, 55-71.

13. Lopez-Puertas, M.; Dinelli, B. M.; Adriani, A.; Funke, B.; Garcia-Comas, M.; Moriconi, M. L.; D'Aversa, E.; Boersma, C.; Allamandola, L. J., Large Abundances of Polycyclic Aromatic Hydrocarbons in Titan's Upper Atmosphere. *Astrophys J* **2013**, *770*.

14. Wilson, E. H.; Atreya, S. K., Chemical Sources of Haze Formation in Titan's Atmosphere. *Planet Space Sci* **2003**, *51*, 1017-1033.

15. Cernicharo, J.; Heras, A. M.; Tielens, A. G. G. M.; Pardo, J. R.; Herpin, F.; Guelin, M.; Waters, L. B. F. M., Infrared Space Observatory's Discovery of C_4H_2, C_6H_2, and Benzene in CRL 618. *Astrophys J* **2001**, *546*, L123-L126.

16. Lovas, F. J.; McMahon, R. J.; Grabow, J. U.; Schnell, M.; Mack, J.; Scott, L. T.; Kuczkowski, R. L., Interstellar Chemistry: A Strategy for Detecting Polycyclic Aromatic Hydrocarbons in Space. *J Am Chem Soc* **2005**, *127*, 4345-4349.

17. Chiar, J. E.; Tielens, A. G. G. M.; Adamson, A. J.; Ricca, A., The Structure, Origin, and Evolution of Interstellar Hydrocarbon Grains. *Astrophys J* **2013**, *770*.

18. Dwek, E., et al., Detection and Characterization of Cold Interstellar Dust and Polycyclic Aromatic Hydrocarbon Emission, from COBE Observations. *Astrophys J* **1997**, *475*, 565-579.

19. Wakelam, V.; Herbst, E., Polycyclic Aromatic Hydrocarbons in Dense Cloud Chemistry. *Astrophys J* **2008**, *680*, 371-383.

20. Kaiser, R. I.; Parker, D. S. N.; Mebel, A. M., Reaction Dynamics in Astrochemistry: Low-Temperature Pathways to Polycyclic Aromatic Hydrocarbons in the Interstellar Medium. *Annu Rev Phys Chem, Vol 66* **2015**, *66*, 43-67.

21. Tielens, A. G. G. M., Interstellar Polycyclic Aromatic Hydrocarbon Molecules. *Annu Rev Astron Astr* **2008**, *46*, 289-337.

22. Tielens, A. G. G. M.; Charnley, S. B., Circumstellar and Interstellar Synthesis of Organic Molecules. *Origins Life Evol B* **1997**, *27*, 23-51.

23. McGuire, B. A.; Burkhardt, A. M.; Kalenskii, S.; Shingledecker, C. N.; Remijan, A. J.; Herbst, E.; McCarthy, M. C., Detection of the Aromatic Molecule Benzonitrile (c-C_6H_5CN) in the Interstellar Medium. *Science* **2018**, *359*, 202-205.

24. Trevitt, A. J.; Goulay, F.; Taatjes, C. A.; Osborn, D. L.; Leone, S. R., Reactions of the CN Radical with Benzene and Toluene: Product Detection and Low-Temperature Kinetics. *J Phys Chem A* **2010**, *114*, 1749-1755.

25. James, P. L.; Sims, I. R.; Smith, I. W. M.; Alexander, M. H.; Yang, M. B., A Combined Experimental and Theoretical Study of Rotational Energy Transfer in Collisions between NO($X\ ^2\Pi_{1/2}$, v = 3, J) and He, Ar and N_2 at Temperatures Down to 7 K. *J Chem Phys* **1998**, *109*, 3882-3897.

26. Sims, I. R.; Queffelec, J. L.; Defrance, A.; Rebrionrowe, C.; Travers, D.; Bocherel, P.; Rowe, B. R.; Smith, I. W. M., Ultralow Temperature Kinetics of Neutral-Neutral Reactions - the Technique and Results for the Reactions CN+O_2 Down to 13 K and CN+NH_3 Down to 25 K. *J Chem Phys* **1994**, *100*, 4229-4241.

27. Gupta, D.; Ely, S. C. S.; Cooke, I. R.; Guillaume, T.; Khedaoui, O. A.; Hearne, T. S.; Hays, B. M.; Sims, I. R., Low Temperature Kinetics of the Reaction between Methanol and the CN Radical. *J Phys Chem A* **2019**, *123*, 9995-10003.

28. Felps, W. S.; Rupnik, K.; Mcglynn, S. P., Electronic Spectroscopy of the Cyanogen Halides. *J Phys Chem* **1991**, *95*, 639-656.

29. O'Halloran, M. A.; Joswig, H.; Zare, R. N., Alignment of CN from 248 nm Photolysis of ICN - a New Model of the a Continuum Dissociation Dynamics. *J Chem Phys* **1987**, *87*, 303-313.

30. Frisch, M. J., et al. *Gaussian 09*, Gaussian, Inc.: Wallingford, CT, USA, 2009.

31. Kendall, R. A.; Dunning, T. H.; Harrison, R. J., Electron-Affinities of the 1st-Row Atoms Revisited - Systematic Basis-Sets and Wave-Functions. *J Chem Phys* **1992**, *96*, 6796-6806.

32. Woon, D. E.; Dunning, T. H., Gaussian-Basis Sets for Use in Correlated Molecular Calculations 3. The Atoms Aluminum through Argon. *J Chem Phys* **1993**, *98*, 1358-1371.

33. Zhao, Y.; Truhlar, D. G., The M06 Suite of Density Functionals for Main Group Thermochemistry, Thermochemical Kinetics, Noncovalent Interactions, Excited States, and Transition Elements: Two New Functionals and Systematic Testing of Four M06-Class Functionals and 12 Other Functionals. *Theor Chem Acc* **2008**, *120*, 215-241.

34. Lee, K. L. K.; McGuire, B. A.; McCarthy, M. C., Gas-Phase Synthetic Pathways to Benzene and Benzonitrile: A Combined Microwave and Thermochemical Investigation. *Phys Chem Chem Phys* **2019**, *21*, 2946-2956.

35. Nakashima, N.; Yoshihara, K., Laser Photolysis of Benzene - 5. Formation of Hot Benzene. *J Chem Phys* **1982**, *77*, 6040-6050.

36. Koban, W.; Koch, J. D.; Hanson, R. K.; Schulz, C., Absorption and Fluorescence of Toluene Vapor at Elevated Temperatures. *Phys Chem Chem Phys* **2004**, *6*, 2940-2945.

37. Kovacs, T.; Blitz, M. A.; Seakins, P. W.; Pilling, M. J., H Atom Formation from Benzene and Toluene Photoexcitation at 248 nm. *J Chem Phys* **2009**, *131*.

38. Woon, D. E., Modeling Chemical Growth Processes in Titan's Atmosphere: 1. Theoretical Rates for Reactions between Benzene and the Ethynyl (C_2H) and Cyano (CN) Radicals at Low Temperature and Pressure. *Chem Phys* **2006**, *331*, 67-76.

39. Zhang, R. M.; Truhlar, D. G.; Xu, X. F., Kinetics of the Toluene Reaction with OH Radical. *Research-China* **2019**, *2019*.

40. Myer, J. A.; Samson, J. A. R., Vacuum-Ultraviolet Absorption Cross Sections of CO, HCl, and ICN between 1050 and 2100 Å. *J Chem Phys* **1970**, *52*, 266-&.

41. Fally, S.; Carleer, M.; Vandaele, A. C., UV Fourier Transform Absorption Cross Sections of Benzene, Toluene, Meta-, Ortho-, and Para-Xylene. *J Quant Spectrosc Ra* **2009**, *110*, 766-782.

42. Hickman, C. G.; Gascooke, J. R.; Lawrance, W. D., The S_1-S_0($^1B_2$-$^1A_1$) Transition of Jet-Cooled Toluene: Excitation and Dispersed Fluorescence Spectra, Fluorescence Lifetimes, and Intramolecular Vibrational Energy Redistribution. *J Chem Phys* **1996**, *104*, 4887-4901.

43. Zimmermann, F. P.; Koban, W.; Roth, C. M.; Herten, D. P.; Schulz, C., Fluorescence Lifetime of Gas-Phase Toluene at Elevated Temperatures. *Chem Phys Lett* **2006**, *426*, 248-251.

44. Lu, K. T.; Eiden, G. C.; Weisshaar, J. C., Toluene Cation - Nearly Free Rotation of the Methyl-Group. *J Phys Chem* **1992**, *96*, 9742-9748.

45. Henis, N. B. H.; Miller, L. L., Mechanism of Gas-Phase Cyanation of Alkenes and Aromatics. *J Am Chem Soc* **1983**, *105*, 2820-2823.

46. Rudolph, H. D.; Dreizler, H.; Jaeschke, A.; Wendling, P., Mikrowellenspektrum Hinderungspotential Der Internen Rotation Und Dipolmoment Des Toluols. *Z Naturforsch Pt A* **1967**, *A 22*, 940-&.

47. Loomis, R. A., et al., Non-Detection of $HC_{11}N$ Towards TMC-1: Constraining the Chemistry of Large Carbon-Chain Molecules. *Mon Not R Astron Soc* **2016**, *463*, 4175-4183.

48. Walsh, C.; Loomis, R. A.; Oberg, K. I.; Kama, M.; van't Hoff, M. L. R.; Millar, T. J.; Aikawa, Y.; Herbst, E.; Weaver, S. L. W.; Nomura, H., First Detection of Gas-Phase Methanol in a Protoplanetary Disk. *Astrophys J Lett* **2016**, *823*.

49. Langston, G.; Turner, B., Detection of ^{13}C Isotopomers of the Molecule HC_7N. *Astrophys J* **2007**, *658*, 455-461.

50. Douberly, G. E.; Ricks, A. M.; Schleyer, P. V. R.; Duncan, M. A., Infrared Spectroscopy of Gas Phase Benzenium Ions: Protonated Benzene and Protonated Toluene, from 750 to 3400 cm^{-1}. *J Phys Chem A* **2008**, *112*, 4869-4874.

51. Joblin, C.; Tielens, A. G. G. M.; Allamandola, L. J.; Geballe, T. R., Spatial Variation of the 3.29 and 3.40 Micron Emission Bands within Reflection Nebulae and the Photochemical Evolution of Methylated Polycyclic Aromatic Hydrocarbons. *Astrophys J* **1996**, *458*, 610-620.

52. Wagner, D. R.; Kim, H. S.; Saykally, R. J., Peripherally Hydrogenated Neutral Polycyclic Aromatic Hydrocarbons as Carriers of the 3 Micron Interstellar Infrared Emission Complex: Results from Single-Photon Infrared Emission Spectroscopy. *Astrophys J* **2000**, *545*, 854-860.

53. Dangi, B. B.; Parker, D. S.; Kaiser, R. I.; Jamal, A.; Mebel, A. M., A Combined Experimental and Theoretical Study on the Gas-Phase Synthesis of Toluene under Single Collision Conditions. *Angew Chem Int Ed Engl* **2013**, *52*, 7186-9.

54. Jones, B. M.; Zhang, F. T.; Kaiser, R. I.; Jamal, A.; Mebel, A. M.; Cordiner, M. A.; Charnley, S. B., Formation of Benzene in the Interstellar Medium. *P Natl Acad Sci USA* **2011**, *108*, 452-457.

55. Wakelam, V., et al., A Kinetic Database for Astrochemistry (KIDA). *Astrophys J Suppl S* **2012**, *199*.

56. Lockyear, J. F.; Fournier, M.; Sims, I. R.; Guillemin, J. C.; Taatjes, C. A.; Osborn, D. L.; Leone, S. R., Formation of Fulvene in the Reaction of C_2H with 1,3-Butadiene. *Int J Mass Spectrom* **2015**, *378*, 232-245.

57. Abeysekera, C.; Joalland, B.; Ariyasingha, N.; Zack, L. N.; Sims, I. R.; Field, R. W.; Suits, A. G., Product Branching in the Low Temperature Reaction of CN with Propyne by Chirped-Pulse Microwave Spectroscopy in a Uniform Supersonic Flow. *J Phys Chem Lett* **2015**, *6*, 1599-1604.

58. Hays, B. M.; Guillaume, T.; Hearne, T. S.; Cooke, I. R.; Gupta, D.; Abdelkdaer Khedaoui, O.; Le Picard, S. D.; Sims, I. R., Design and Performance of an E-Band Chirped Pulse Spectrometer for Kinetics Applications: OCS - He Pressure Broadening. *J Quant Spectrosc Ra* **2020**, *250*.